Seasonal oscillations of middle atmosphere temperature observed by Rayleigh lidars and their comparisons with TIMED/SABER observations

Xiankang Dou, Tao Li, Jiyao Xu, Han-Li Liu, Xianghui Xue, Shui Wang, Thierry Leblanc, I. Stuart Mcdermid, Alain Hauchecorne, Philippe Keckhut, et al.

Seasonal oscillations of middle atmosphere temperature observed by Rayleigh lidars and their comparisons with TIMED/SABER observations

Xiankang Dou,[1] Tao Li,[1] Jiyao Xu,[2] Han-Li Liu,[3] Xianghui Xue,[1] Shui Wang,[1] Thierry Leblanc,[4] I. Stuart McDermid,[4] Alain Hauchecorne,[5] Philippe Keckhut,[5] Hassan Bencherif,[6] Craig Heinselman,[7] Wolfgang Steinbrecht,[8] M. G. Mlynczak,[9] and J. M. Russell III[10]

Received 22 December 2008; revised 15 June 2009; accepted 9 July 2009; published 17 October 2009.

[1] The long-term temperature data sets obtained by Rayleigh lidars at six different locations from low to high latitudes within the Network for the Detection of Atmospheric Composition Change (NDACC) were used to derive the annual oscillations (AO) and semiannual oscillations (SAO) of middle atmosphere temperature: Reunion Island (21.8°S); Mauna Loa Observatory, Hawaii (19.5°N); Table Mountain Facility, California (34.4°N); Observatoire de Haute Provence, France (43.9°N); Hohenpeissenberg, Germany (47.8°N); Sondre Stromfjord, Greenland (67.0°N). The results were compared with those derived from the Sounding of the Atmosphere using Broadband Emission Radiometry (SABER) instrument onboard the Thermosphere-Ionosphere-Mesosphere Energetics and Dynamics (TIMED) satellite. The zonal mean temperatures at similar latitudes show good agreement. The observations also reveal that the AO dominates the seasonal oscillations in both the stratosphere and the mesosphere at middle and high latitudes, with the amplitudes increasing poleward. The SAO oscillations are weaker at all six sites. The oscillations in the upper mesosphere are usually stronger than those in the upper stratosphere with a local minimum near 50–65 km. The upper mesospheric signals are clearly out of phase with upper stratospheric signals. Some differences between lidar and SABER results were found in both the stratosphere and mesosphere. These could be due to: the difference in data sampling between ground-based and space-based instruments, the length of data set, the tidal aliasing owing to the temperature AO and SAO since lidar data are nighttime only, and lidar temperature analysis algorithms. The seasonal oscillations of tidal amplitudes derived from SABER observations suggests that the tidal aliasing of the lidar temperature AO and SAO in the upper mesosphere may over- or under-estimate the real temperature oscillations, depending on the tidal phases. In addition, the possibly unrealistic seasonal oscillations embedded in the climatological models (e.g., MSIS or CIRA) at the reference point for lidar temperature analysis may also affect the lidar results in the top part of the profiles (usually in the upper mesosphere).

Citation: Dou, X., et al. (2009), Seasonal oscillations of middle atmosphere temperature observed by Rayleigh lidars and their comparisons with TIMED/SABER observations, *J. Geophys. Res.*, *114*, D20103, doi:10.1029/2008JD011654.

[1]Mengcheng National Geophysical Observatory, School of Earth and Space Sciences, University of Science and Technology of China, Hefei, China.
[2]Key Laboratory for Space Weather, Chinese Academy of Sciences, Beijing, China.
[3]High Altitude Observatory, National Center for Atmospheric Research, Boulder, Colorado, USA.
[4]Table Mountain Facility, Jet Propulsion Laboratory, California Institute of Technology, Wrightwood, California, USA.
[5]Service d'Aéronomie, Institut Pierre-Simon Laplace, CNRS, Verrières-le-Buisson, France.
[6]Laboratoire de l'Atmosphère et des Cyclones, Université de La Réunion, Saint-Denis, France.
[7]SRI International, Menlo Park, California, USA.
[8]Meteorological Observatory Hohenpeissenberg, German Weather Service, Hohenpeissenberg, Germany.
[9]NASA Langley Research Center, Hampton, Virginia, USA.
[10]Center for Atmospheric Sciences, Hampton University, Hampton, Virginia, USA.

0148-0227/09/2008JD011654

1. Introduction

[2] The seasonal oscillations of middle atmosphere temperature, such as the annual oscillation (AO) and the semiannual oscillation (SAO), have been studied for decades using climatological data sets [*Reed*, 1962; *Hamilton*, 1982; *Garcia et al.*, 1997; *Leblanc et al.*, 1998a; *Randel et al.*, 2004]. The early satellite observations showed that the SAO is the dominant seasonal variation in both wind and temperature in the tropical middle atmosphere [*Delisi and Dunkerton*, 1988; *Garcia and Clancy*, 1990]. The stratospheric SAO (SSAO) peaks near the stratopause, while the mesospheric SAO (MSAO) peaks near the mesopause, with minimum SAO amplitude near ~65 km, as suggested by rocketsonde observations [*Hirota*, 1978]. The observations also found that the SSAO near the stratopause is almost 180 degree out of phase with MSAO near the mesopause [*Hirota*, 1978; *Hamilton*, 1982]. It is believed that the MSAO is primarily driven by gravity and Kelvin waves which are selectively filtered by the SSAO wind leading to the out-of-phase feature of the MSAO with the SSAO [*Dunkerton*, 1982; *Sassi and Garcia*, 1997; *Richter and Garcia*, 2006]. The AO dominates seasonal variations in the middle atmosphere at middle and high latitudes, with a weaker peak in the stratosphere and a stronger peak in the mesosphere, and the stratospheric oscillations are out of phase with those in the mesosphere [*Remsberg et al.*, 2002; *Xu et al.*, 2007].

[3] Using four Rayleigh lidar data sets, *Leblanc et al.* [1998a] derived the AO and SAO of middle atmosphere temperature from low to middle latitudes and compared the results with the CIRA-86 model. Since most of lidar systems only operate for a number of hours in the nighttime, tidal oscillations are quite evident in the lidar data sets [*Leblanc et al.*, 1999; *Morel et al.*, 2002; *Haefele et al.*, 2008], but they could not be determined accurately with these nighttime limited data [*Crary and Forbes*, 1983]. The AO and SAO of tidal waves may therefore cause significant tidal aliasing to the temperature AO and SAO derived from nighttime data sets, especially in the mesosphere where the tides grow strong enough to dominate the wave oscillations [*Garcia and Clancy*, 1990; *Keckhut et al.*, 1996; *Garcia et al.*, 1997]. *Zhao et al.* [2007] presented the upper mesospheric temperature AO and SAO measured by OH and O_2 all-sky imagers over Maui, Hawaii and, with the help of TIME-GCM simulation, suggested that the diurnal tide aliasing of the SAO derived from nighttime data could be as strong as ~5 K near 87 km.

[4] In this paper, the long-term observations of middle atmospheric temperature by six Rayleigh lidars located from low to high latitudes within the Network for the Detection of Atmospheric Composition Change (NDACC) [*Keckhut et al.*, 2004] were used to study the temperature AO and SAO in the middle atmosphere. Wherever available, the lidar results were also compared with those derived from coincident temperature measurements from the Sounding of the Atmosphere using Broadband Emission Radiometry (SABER) instrument onboard the Thermosphere-Ionosphere-Mesosphere Energetics and Dynamics (TIMED) satellite. The description of instruments, data sets, and data analysis methods will be presented in section 2, followed by the vertical profiles of mean temperatures and AO and SAO observed by lidar and SABER in section 3. Section 4 will discuss the differences between the different sites and the possible aliasing of lidar seasonal oscillations owing to tidal waves and lidar temperature analysis algorithms. A conclusion will be drawn in section 5.

2. Instruments, Data Sets, and Data Analysis

[5] The Rayleigh lidar collects the laser photons backscattered by air molecules in the middle atmosphere. The temperature profile derived from Rayleigh lidar usually starts at ~30 km where the aerosol backscattering is negligible compared to air molecule backscattering [*Hauchecorne and Chanin*, 1980]. Owing to both the exponential decrease of air density and $1/z^2$ dependence of lidar signal with altitude z, the Rayleigh backscattering signals are also decreased, leading to larger measurement uncertainty at the higher altitudes especially in the mesosphere. To retrieve temperature, an initial value is needed at a reference point at the top of profile (usually obtained from climatological mode; e.g., MSIS or CIRA) to derive the temperature vertical profile through downward integration. The uncertainties caused by initial value can strongly affect the temperature derivation in the top 10–15 km of the profile but has negligible influence below this [*Leblanc et al.*, 1998b]. Therefore, this large uncertainty may contaminate the derivation of the AO and SAO in the upper mesosphere.

[6] The six Rayleigh lidar temperature data sets (nighttime mean) from the NDACC lidar network were downloaded from the NDACC website at http://www.ndsc.ncep.noaa.gov/. Table 1 lists the characteristics of each lidar data set. These long-term data sets with more than 10 years duration cover the different latitudes from Reunion Island in the southern hemisphere (REU, 21.8°S), to Mauna Loa Observatory, Hawaii (MLO, 19.5°N), and Table Mountain Facility, California (TMF, 34.4°N) in the lower latitudes, Observatoire de Haute Provence (OHP, 43.9°N) and Hohenpeissenberg (HOH, 47.8°N) in the middle latitudes, and Sondre Stromfjord, Greenland (SFJ, 67.0°N) at high latitude. Each lidar system is usually operated for a number of hours depending on the system and weather conditions, with more regular operation (2 h per night) at both MLO and TMF. All the lidar systems have already accumulated more than 1000 profiles, except the SFJ lidar. Using the 14-year-long MLO lidar data set (the same data set as used in this paper), *Li et al.* [2008a] studied the interannual variability of middle atmosphere temperature over Hawaii Island with first time observation of the strong temperature response to El Niño–Southern Oscillation in the middle mesosphere. Figure 1 shows a histogram of the number of profiles in each month for six lidar sites. It is clear that the SFJ lidar data set has a lower number of profiles than any other data sets, especially in the summer months owing to the summer polar day preventing lidar observations. To derive the AO and SAO from the lidar data sets we first regroup the temperature profiles according to their UT day regardless of the year to form a composite year of data. We then decompose this newly formed data set to its mean, plus one-year and half-year period components. The uncertainty (error bars) of AO and SAO amplitudes and phases were estimated according to the variances and covariances obtained from least squares fits. We virtually checked the

Table 1. Characteristics of the Six Rayleigh Lidar Data Sets

Data Sets	Latitude, Longitude	Duration	Regular Operating Hours per Night	Total Number of Profiles
REU	22°S, 55°E	1994–2006	2–10	1058
MLO	19.5°N, 55.6°W	1994–2007	2	1903
TMF	34.4°N, 117.7°W	1989–2007	2	1929
OHP	44°N, 6°E	1991–2007	4–10	2332
HOH	47.8°N, 11°E	1988–2007	4–10	1790
SFJ	67°N, 51°W	1994–2007	3–10	502

fitting at several representative altitudes (not shown), and good fitting could be clearly seen. As an example, we show in Figure 2 the time series of raw temperature and their corresponding fitting at four altitudes, 20, 40, 60, and 80 km, observed by lidar at MLO. The reasonably good fitting could be clearly seen, suggesting that the AO and SAO dominate the seasonal oscillations of middle atmosphere temperature at MLO and that the residual variation is entirely on short time scales. The AO and SAO oscillations revealed by lidars could explain as large as 60–80% of total variances in the stratosphere and less than 60% in the mesosphere. This is most likely due to increased statistical uncertainty from stratosphere to mesosphere.

[7] The TIMED satellite was launched on 7 December 2001. As one of four key instruments onboard TIMED, SABER measured the temperature profile from the lower stratosphere to the lower thermosphere, daily and near globally for the first time. It also measures O_3, H_2O and CO_2 mixing ratio vertical profiles and key energetic parameters describing upper atmosphere heating, cooling and airglow losses [*Russell et al.*, 1999]. Temperature is measured using three channels in the 15 and 4.3 μm CO_2 bands while the remaining seven SABER channels cover the range from 1.27 to 9.6 μm. The scientific data measured by SABER, including temperatures in the middle atmosphere, have been available since January 2002. The effective vertical resolution of SABER temperature was estimated to be ~2 km in the stratosphere and mesosphere [*Remsberg et al.*, 2003]. To study the annual and semiannual oscillations, we used the SABER temperature data set version 1.07 from January 2002 through September 2008.

[8] The TIMED satellite is nearly sun synchronous and orbits Earth ~15 times a day with descending and ascending data points separated by ~10 h. It takes roughly 60 days to complete a maximum of ~22 h local time coverage. Since the global structure of the AO and SAO have been shown in detail by *Xu et al.* [2007], in this paper we only present the results at the latitude of each lidar site for

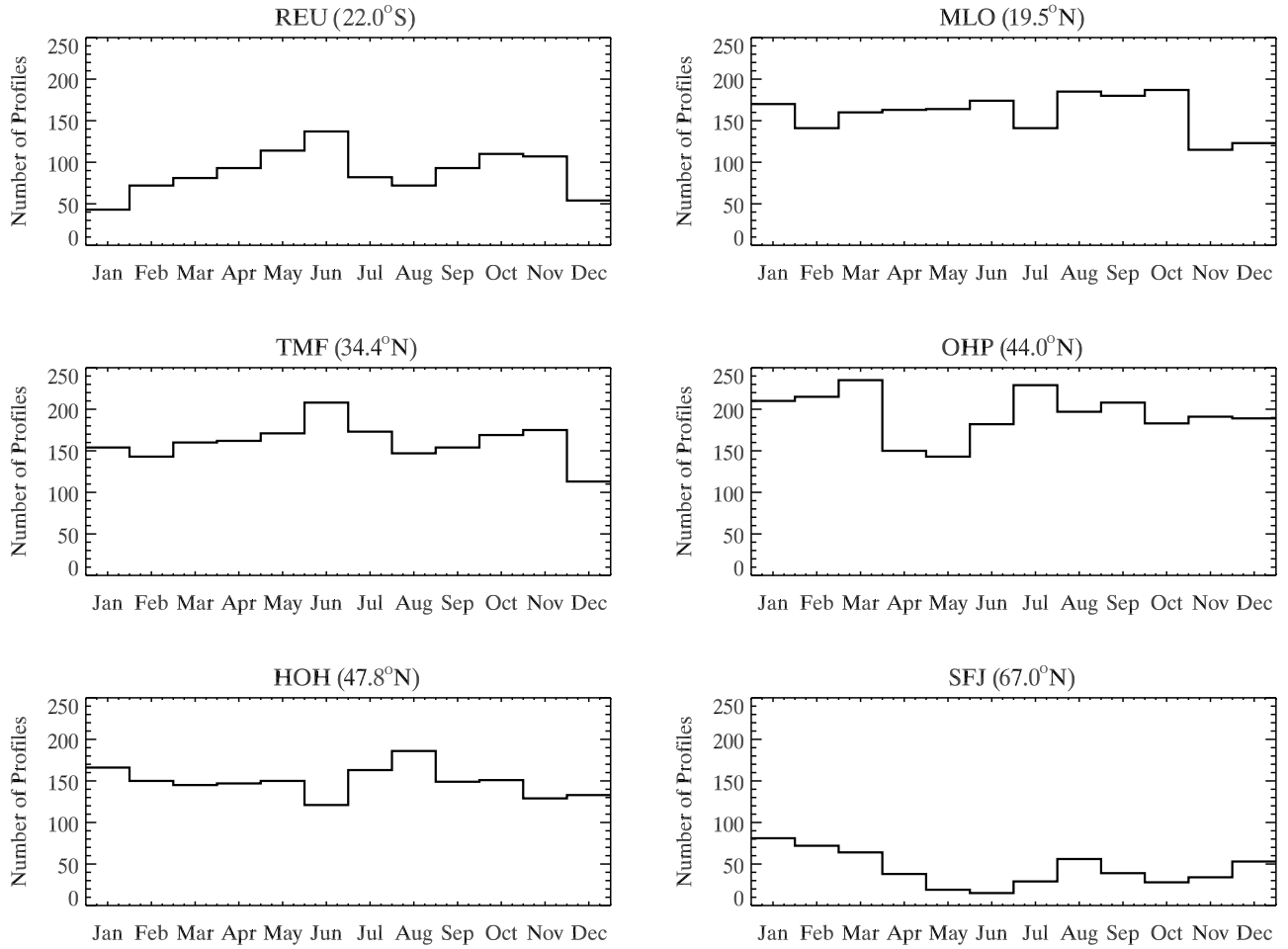

Figure 1. Histogram of the number of profiles for each lidar data set.

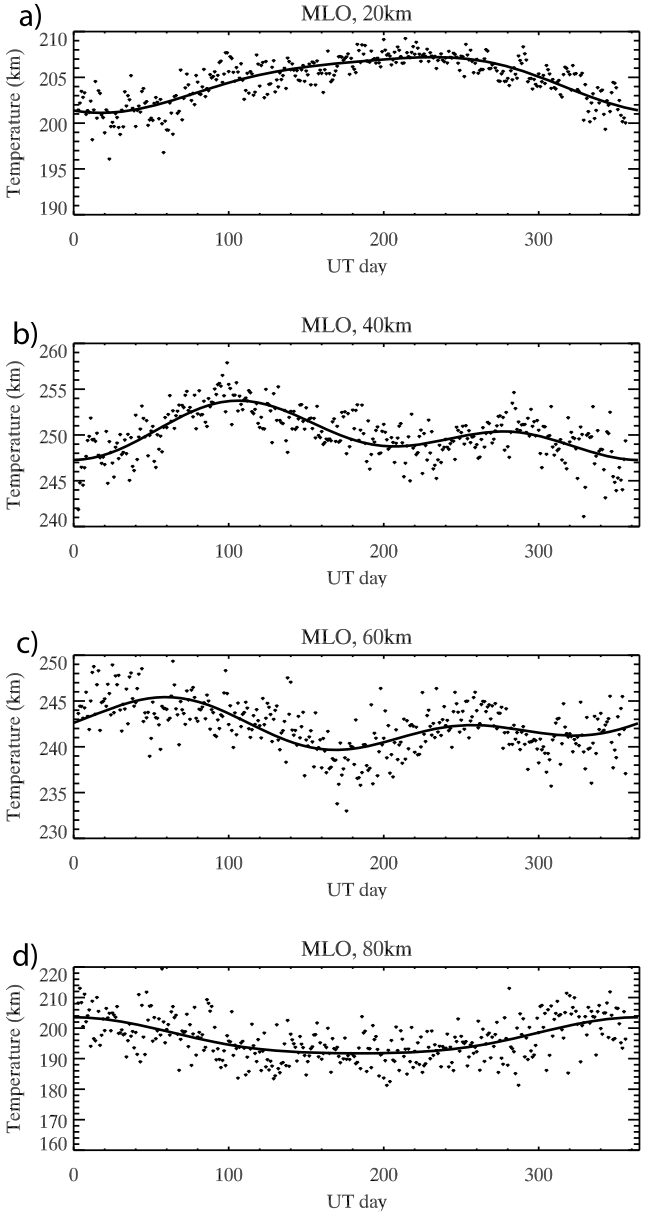

Figure 2. The time series of raw temperature and their corresponding fitting at four different altitudes: (a) 20 km, (b) 40 km, (c) 60 km, and (d) 80 km observed by lidar at MLO.

comparison. Prior to data analysis, we interpolated the SABER raw temperature profiles (V1.07 with non-LTE included in the upper mesosphere) by fitting on a minimum curvature surface to form a regular longitude data grid with 15° wide at the latitude of each lidar site, and then derived the ascending and descending daily zonal mean temperature by just averaging all the ascending and descending points available in this UT day, respectively. Within 60-day window, we first re-sorted the daily zonal mean temperature (including both ascending and descending daily mean) with their local time and then linear-square fitted them at each altitude with the mean and 24-, 12-, and 8-h tidal components. The obtained mean is defined here as SABER 60-day zonal mean temperature with tidal waves removed. The detailed description of this method and their corresponding equations could be found in the work of *Xu et al.* [2007]. To derive the AO and SAO amplitudes and phases, we finally decomposed the SABER 60-day zonal mean temperature obtained from above method at the latitude of each lidar site to a mean plus one-year and half-year period components. Since the tidal waves were removed prior to the derivation of the AO and SAO, the tidal aliasing of the temperature AO and SAO was then minimized. On the other hand, the diurnal (24 h) and semidiurnal (12 h) tides derived from the 60-day windows could also be used to assess the tidal aliasing of the temperature AO and SAO derived from the lidar data sets.

3. Results

[9] Figure 3 shows the amplitudes and phases of the AO (solid lines) and SAO (dotted lines) derived from lidar (blue lines) and SABER (red lines) data sets at (top) REU, (middle) MLO, and (bottom) TMF and the corresponding amplitude difference between lidar and SABER. It is clear that in the subtropical latitudes (REU and MLO), the SAO and AO observed by lidar and SABER both show small amplitudes of less than 2 K below 60 km, and around 2–4 K above, and the amplitude difference between lidar and SABER is less than 2 K at most of altitudes for both AO and SAO. The phases of the AO and SAO observed by both lidar and SABER show downward progression. The MSAO near 80 km is roughly out of phase with the SSAO near 50 km, consistent with the SAO feature in the tropics revealed early by satellite observations [*Delisi and Dunkerton*, 1988]. The phases observed by lidar at REU at most altitudes were sporadic especially for the SAO, while the lidar results at MLO are quite smooth and agree very well with SABER results at most altitudes up to ~80 km. This may be because the REU lidar operated at 532 nm, with ~3 W output power and a smaller receiver of ~0.53 m diameter [*Baray et al.*, 1999; D. Faduilhe et al., First climatology of Rayleigh lidar temperature over a tropical station in the Southern Hemisphere, submitted to *Journal of Atmospheric and Solar-Terrestrial Physics*, 2008], while the MLO system operated at 355 nm, with ~8–10 W output laser power and 1 m diameter receiver [*McDermid et al.*, 1995]. As a result, the lidar signal-to-noise ratio at MLO is much higher than that at REU. Furthermore, at MLO the lidar observed SAO phases between 50 and 60 km are leading SABER phases by 1–3 months, corresponding to the smaller SAO amplitude of ~0.5 K. We also noted that the REU and MLO are near the nodal point of diurnal tide [*Forbes*, 1995], so the aliasing from diurnal tide should be small. And also the temperature data below 30 km at MLO were retrieved from Raman channel.

[10] At TMF (Figure 3, bottom), the SAO observed by both lidar and SABER shows much smaller amplitude of less than 0.5 K in the stratosphere, and relatively stronger amplitude of 2–4 K in mesosphere with two peaks of ~4 K near 60 and 75 km, respectively. The SAO phase plot indicates that the two peaks in the mesosphere are out of phase. Compared to the SAO, the observed AO is much stronger in both the stratosphere and the mesosphere, with one maximum in the middle stratosphere and the other in the upper mesosphere. The minimum amplitude of the AO near 60–65 km observed by lidar is ~3 km lower than that

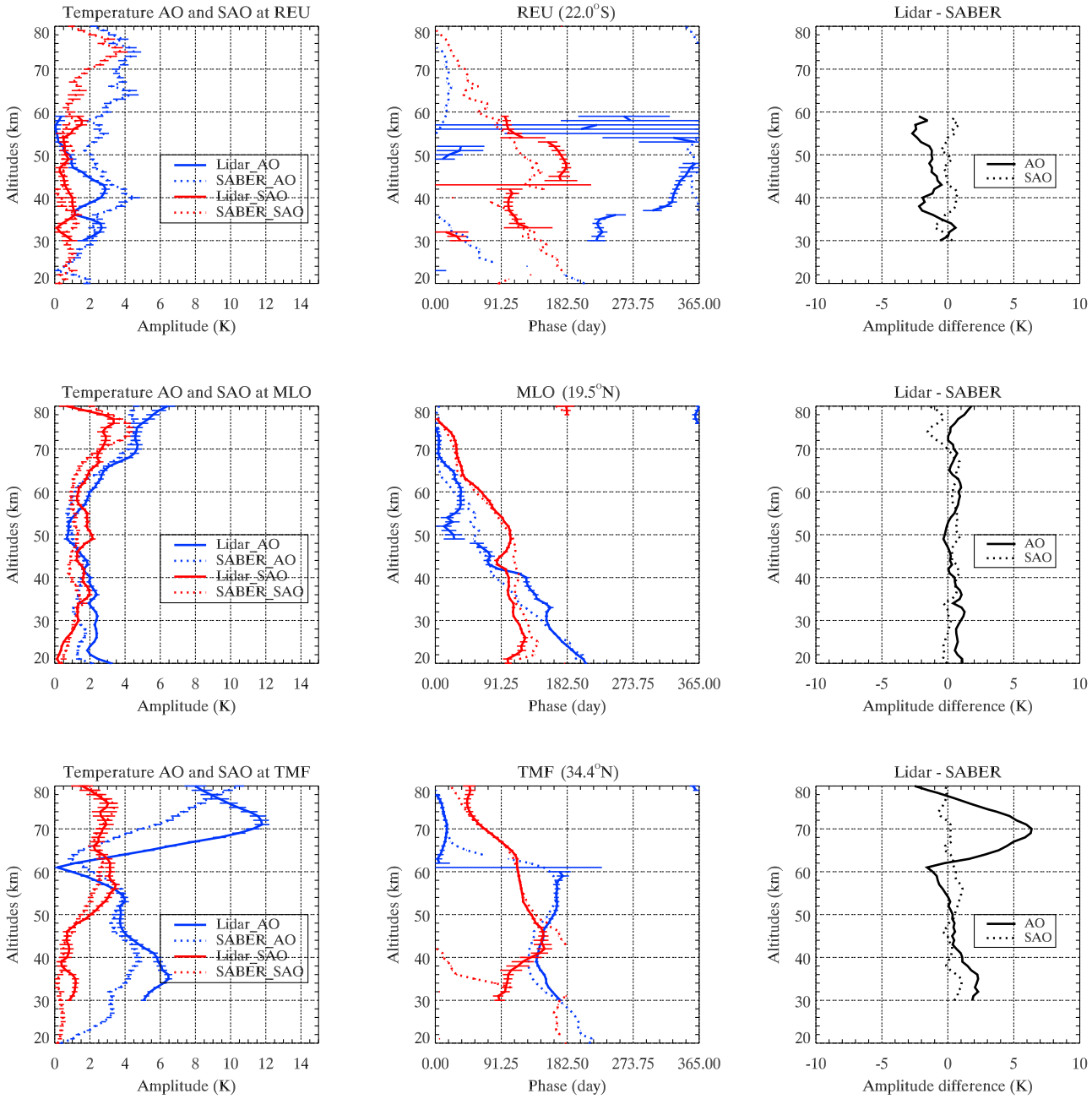

Figure 3. Amplitudes and phases of the AO (blue lines) and SAO (red lines) observed by lidar (solid lines) and SABER (dotted lines) and the amplitude differences between lidar and SABER at (top) REU, (middle) MLO, and (bottom) TMF.

observed by SABER. The AOs below 60 km (peak near the summer time) are out of phase with the AOs above (peak near the winter time). Although the comparisons between lidar and SABER results show good agreement, the lidar observed amplitudes are slightly greater than those observed by SABER, especially for the AO in the mesosphere with ~5 K difference, possibly indicating tidal aliasing of the lidar results. On the other hand, the AO and mesospheric SAO at TMF are stronger than those at the two subtropical lidar sites (REU and MLO). The AO is clearly stronger than the SAO at TMF, while two oscillations are comparable at REU and MLO.

[11] Similar to Figure 3, Figure 4 shows the amplitudes and phases of the AO and SAO derived from lidar and SABER data sets at two midlatitude (OHP and HOH) and one high-latitude (SFJ) sites. At OHP, the SAO observed by lidar with two out-of-phase peaks near 40 and 65 km is ~2 K larger than that observed by SABER, while the lidar observed AO is about 2–4 K weaker than that observed by SABER in both the stratosphere and mesosphere. The stronger SAO derived from lidar data set could be due to aliasing from diurnal tide, because the subpeak of diurnal tide in temperature is at midlatitudes [*Forbes*, 1995]. This is also true for the AO and SAO observed at HOH, though the

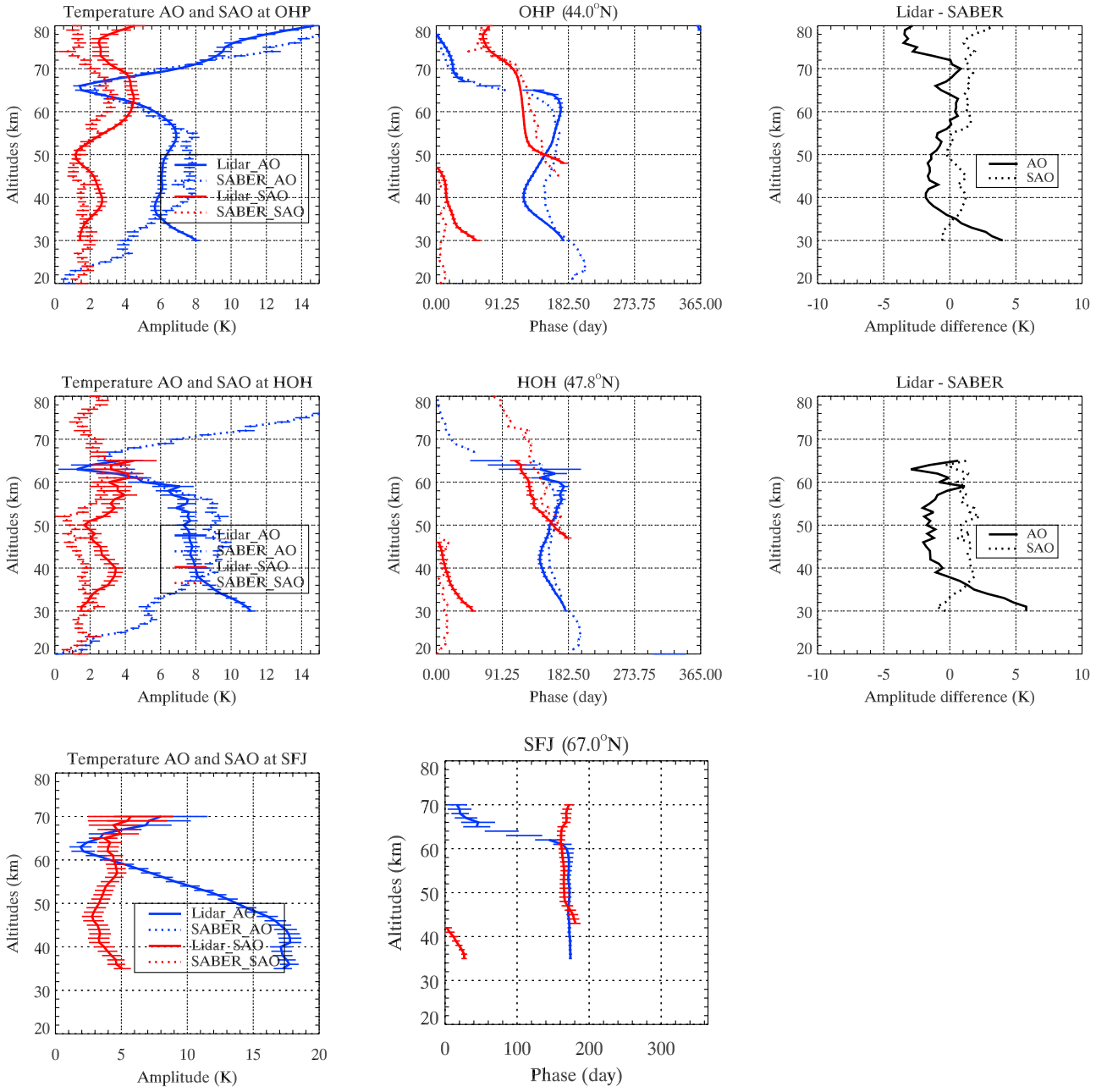

Figure 4. Same as Figure 3 except for OHP, HOH, and SFJ. There is no SABER result available at SFJ.

HOH lidar results only reach ~65 km. The AOs at OHP and HOH are clearly stronger than those at lower latitudes. Since the analysis of SABER was limited between −55° to 55° latitudes without data gaps owing to satellite yaw orbits, we present only the lidar observed AO and SAO at SFJ (67°N). In the stratosphere, the SAO at SFJ with amplitudes of 5–7 K was still one third as strong as the AO with amplitude of 15–20 K, with both oscillations stronger than those at midlatitude. Finally, it is also clearly presented in Figures 3 and 4 that the AO is the dominant seasonal oscillation in the middle atmosphere temperature in the both middle and high latitudes, consistent with the satellite observations [*Xu et al.*, 2007].

[12] Figure 5 shows the mean temperature profiles derived from long-term lidar and SABER data sets illustrating generally good agreement. However, a clear difference was found in the stratosphere with warmer lidar temperatures near stratopause and colder below 40 km. The difference of mean temperature between lidar and SABER in the stratosphere may possibly due to either a bias in SABER temperature, or tidal aliasing and/or the presence of sporadic aerosols leading to introduce a cold bias in lidar temperature. It is also worthwhile to mention that at MLO the lidar observed temperatures are clearly ~2–5 K colder than SABER temperature between 40 and 15 km. This could also be partly caused by diurnal tidal aliasing: the phase of

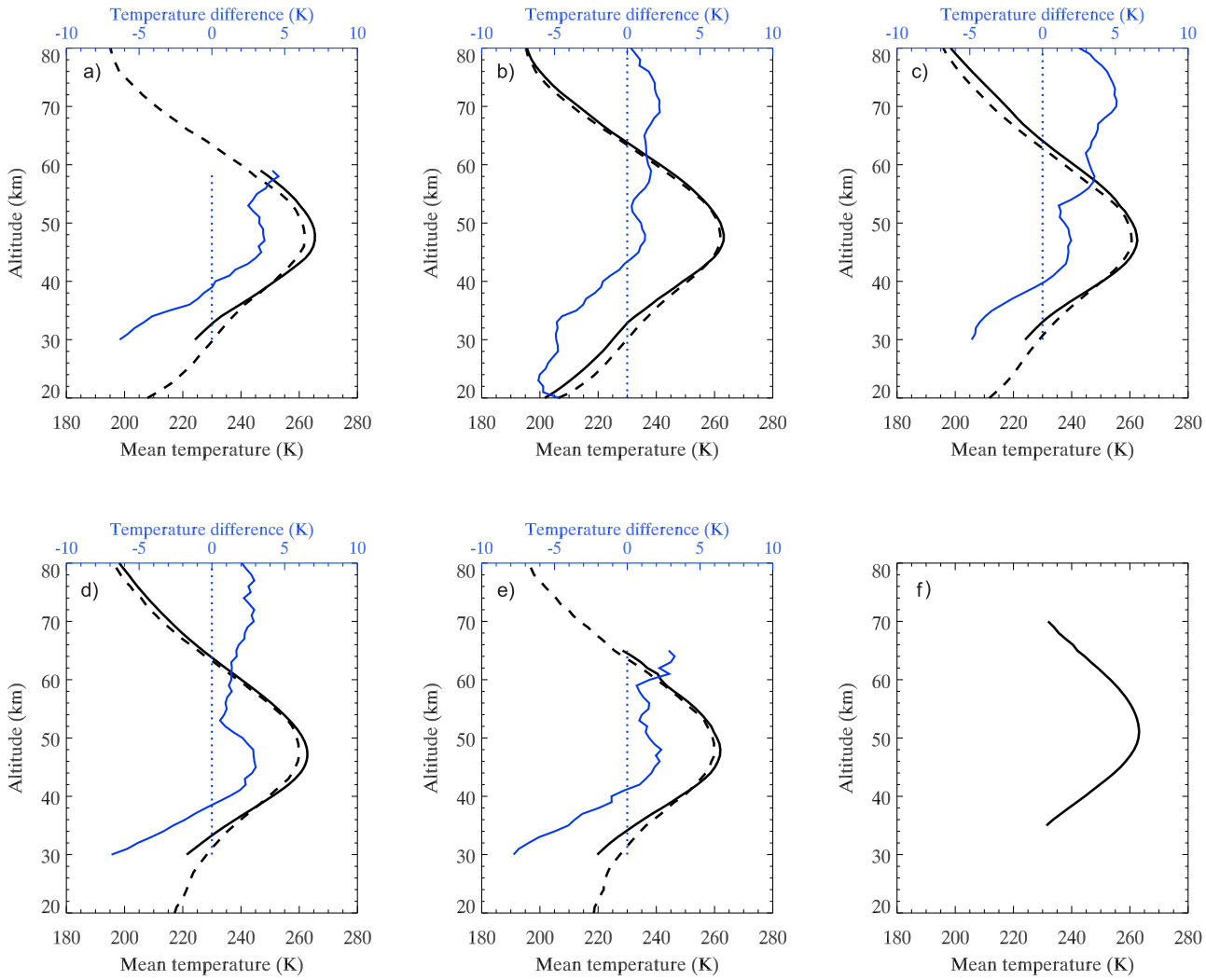

Figure 5. The mean temperature observed by lidar (solid lines) and SABER (dotted lines) at (a) REU, (b) MLO, (c) TMF, (d) OHP, (e) HOH, and (f) SFJ, as well as their differences (blue lines).

diurnal temperature near 30 km at 20 N is in early afternoon (not shown). As a result, the nocturnal lidar measurements will sample the cold phase of the diurnal tide at MLO and thus have a cold bias in lidar temperature. Both lidar and SABER observations revealed the stratopause is located at ~46–48 km in the low and middle latitudes and ~51 km at high latitude, consistent with increased stratopause altitudes from low to high latitudes from model simulations [*Baldwin et al.*, 2001].

4. Discussion

[13] The lidar and SABER results for the temperature AO and SAO generally show good agreements but with some differences found in both the stratosphere and mesosphere. We note that the vertical resolution of lidar temperature was variable with less than 1 km in the stratosphere and increased to 5–10 km in the upper mesosphere in order to increase the signal-to-noise ratio [*Keckhut et al.*, 2004]; while the effective vertical resolution of SABER temperature was ~2 km [*Remsberg et al.*, 2003] in the stratosphere and mesosphere. The different resolutions between lidar and SABER temperature profiles may partially cause the difference of derived seasonal oscillations. However, the difference in the upper mesosphere could be due to the tidal aliasing of the AO and SAO caused by nighttime only lidar data, which was addressed in the early literature [*Garcia et al.*, 1997; *Zhao et al.*, 2007], and due to the difference in sampling data between ground-based and space-based instruments [*Li et al.*, 2008b], as well as the length of data set and larger uncertainties at higher altitudes. The SABER results were derived from zonal mean temperature with prior removal of tides. As a result, the tidal aliasing or contamination of SABER temperature AO and SAO was believed to be minimized [*Xu et al.*, 2007]. Using the migrating tidal results extracted from the SABER data within 60-day windows, we are able to assess the tidal aliasing to lidar temperature AO and SAO by evaluating the seasonal oscillations of tides.

[14] Figure 6 shows the AO (blue lines) and SAO (red lines) amplitudes and phases of migrating diurnal (solid lines) and semidiurnal (dotted lines) amplitudes derived from SABER at (top) MLO, (middle) TMF, and (bottom) OHP. The AO and SAO of both diurnal and semidiurnal

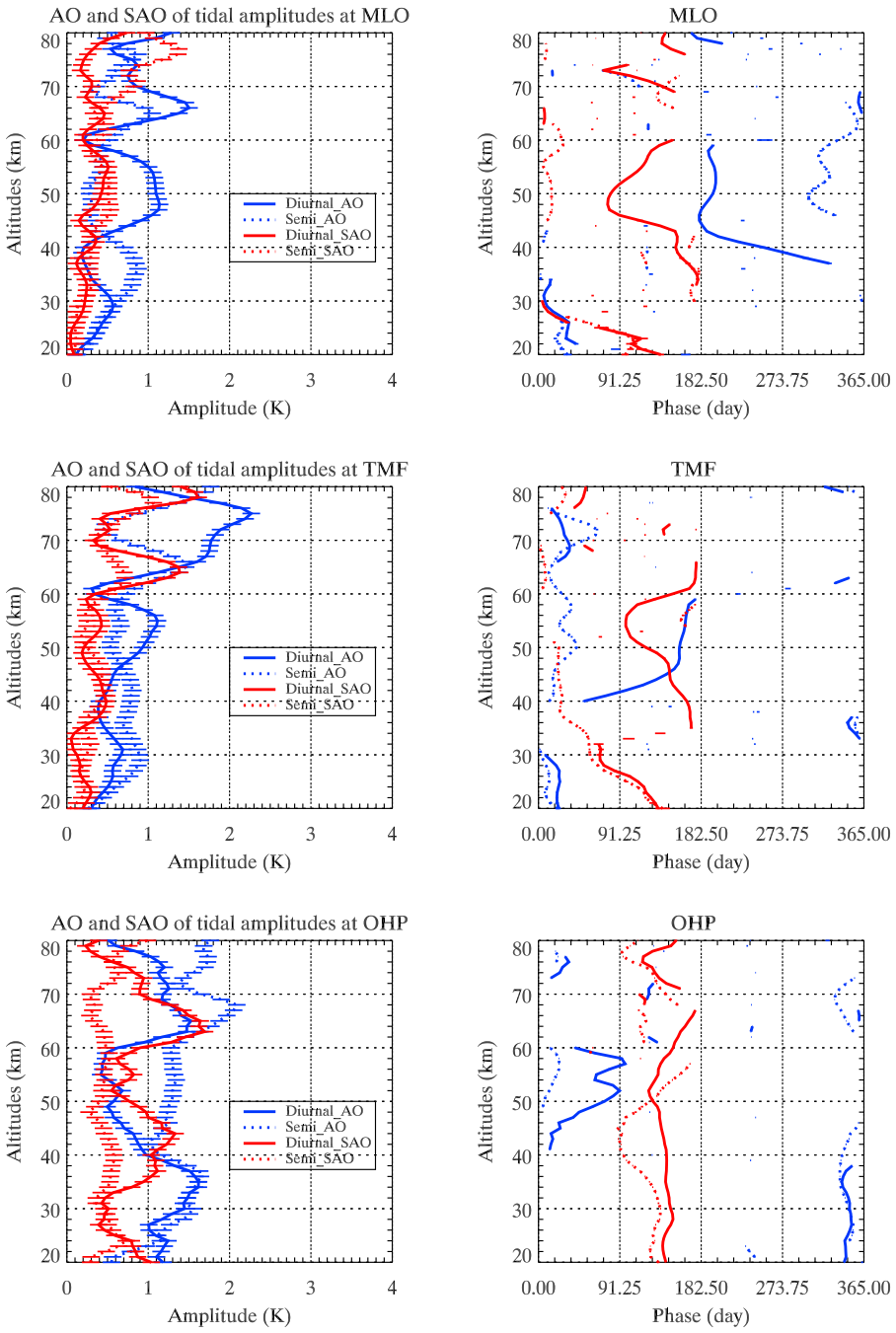

Figure 6. Amplitudes and phases of the AO (blue lines) and SAO (red lines) of migrating diurnal (solid lines) and semidiurnal (dotted lines) amplitudes derived from SABER at (top) MLO, (middle) TMF, and (bottom) OHP.

amplitudes at MLO are around or less than 1 K, with a local maximum of ~1.2 K near 50 and 65 km. The AO phase of diurnal amplitude at 65 km is generally in phase with temperature AO (see MLO phase in Figure 3, middle). The small diurnal and semidiurnal amplitudes at MLO lead to less difference between lidar and SABER observed temperature AO and SAO (see MLO amplitude in Figure 3, middle). As a result, the tidal aliasing could be negligible. The small tidal amplitudes at MLO (near 20°N latitude) we derived are consistent with the classic GSWM model [*Hagan and Forbes*, 2002] and other derivation methods for SABER observations [*Zhang et al.*, 2006].

[15] The diurnal amplitude of the AO at TMF (near 34N latitude), however; increases to ~2.3 K near 75 km, twice as large as that at MLO, consistent with the distribution of the Hough function at midlatitudes [*Forbes*, 1995]. This maximum AO amplitude of diurnal oscillation corresponds to the large temperature AO difference between lidar and SABER, and also in phase with temperature AO, suggesting diurnal perturbation aliasing to the lidar results. Since the TMF lidar usually operates for 2 h starting at ~1900–

2100 LT (end of astronomical twilight), seasonal oscillations of both diurnal and semidiurnal tides could strongly affect the derivation of the temperature AO and SAO. The derived diurnal phases at 70–80 km between 2002 and 2008 are variable with season from 1500 to 2000 LT (not shown), consistent with the GSWM model and *Zhang et al.*'s [2006] results. Therefore, the AO oscillation induced solely by the migrating diurnal tide could reach as high as ~2 K near 75 km, which should be able to reduce the difference between lidar and SABER derived temperature AO amplitudes. This is similar to the tidal aliasing discussed by *Zhao et al.* [2007] in the mesopause region temperature seasonal oscillations revealed by nighttime temperature mapper measurements over Maui, HI.

[16] Similar to TMF, the tidal amplitudes at the midlatitude site OHP show stronger seasonal oscillations than those at MLO. While different from TMF, the semidiurnal AO amplitude is slightly greater than the diurnal AO amplitude for most altitudes above 40 km. Two local maxima were found to be ~2.3 and ~1.5 K near 68 and 38 km, respectively. The most significant difference between lidar and SABER results is located in the upper stratosphere and upper mesosphere. Above 70 km, the diurnal phases between 2002 and 2008 are generally variable from 1300 to 1800 LT with seasons, while the semidiurnal phases are variable from 0300 to 0700 LT (not shown). Since the OHP lidar system was usually operated for more than 4 h, sometimes overnight, the semidiurnal aliasing to seasonal oscillation derived from these data is reduced. However, this is not case for the diurnal tide aliasing to the lidar temperature season oscillations. According to the SABER derived diurnal phase, the perturbation above 70 km induced by diurnal tide at midnight is negative. The temperature AO (peak in January) revealed in Figure 4 (top) approximately lag behind the diurnal amplitude AO (peak in December) by 1–2 months, while the temperature SAO is almost out of phase with diurnal amplitude SAO, leading to the underestimation of lidar temperature AO and over-estimation of lidar temperature SAO.

[17] As pointed out previously, the lidar temperature profiles were retrieved by setting up the initial values at a reference point near the top of the profile (usually obtained from climatological model e.g., MSIS or CIRA) and then performing downward integration [*Hauchecorne and Chanin*, 1980]. *Leblanc et al.* [1998b] found that an initial reference temperature 15 K warmer at 90 km than the true value could induce ~5 K warmer at 80 km, only due to the lidar temperature analysis algorithms. As a result, possible unrealistic seasonal oscillations embedded in the climatological model at the reference point may affect the apparent lidar temperature seasonal oscillations, at least, on the top part of the profiles. Depending on the signal-to-noise ratio of lidar return signals, the reference points for OHP, TMF, and MLO were usually located between 80 and 95 km.

[18] To explore the possible aliasing induced by an unrealistic initial value at the reference altitude, in Figure 7 we plotted the temperature AO (blue lines) and SAO (red lines) derived from SABER (dotted lines) and MSIS-90 model (solid lines) between 80 and 90 km. The MSIS AO and SAO amplitudes at all three sites are clearly stronger than those derived from SABER measurements, except for SAO at MLO, while the MSIS phases generally agree very well with SABER phases, except for MLO. At TMF, the MSIS AO oscillation is around 4 K stronger than SABER AO, leading to the over-estimation of lidar AO in the region below 80 km. The SABER observations show quite smaller SAO with the phase shifted by 180° near 82 km at both TMF and OHP, while MSIS presents a stronger SAO oscillation without phase shift. This may cause bias to lidar derived temperature SAO above 70 km. As noted in Figures 3 and 4, we indeed see the lidar temperature SAO at TMF and OHP are clearly stronger than those derived from SABER zonal mean temperature. However, at OHP the MSIS temperature AO is fairly close to the SABER temperature AO below 84 km, indicating that the difference between lidar AO and SABER AO may not be caused by lidar temperature analysis algorithms, may be caused by other reasons, e.g., the length of the data set and different sampling methods.

5. Summary

[19] Using the long-term temperature data sets observed by six Rayleigh lidars (REU, MLO, TMF, OHP, HOH, and SFJ) from low (20°S, 20°N) to middle (34°N, 44°N, and 47°N) and high (67°N) latitudes within the NDACC network, we derived the temperature AO and SAO oscillations in the stratosphere and mesosphere. The lidar results were also compared with those derived from the SABER zonal mean temperatures (2002–2008). We found that the AO oscillations dominate the seasonal oscillations in both stratosphere and mesosphere at middle and high latitudes with the amplitudes increasing poleward, while the SAO oscillations are weaker at all six sites. The oscillations in the upper mesosphere are usually stronger than those in the upper stratosphere with a local minimum near 50–65 km. The upper mesospheric signals are clearly out of phase with upper stratospheric signals. All these features of seasonal oscillations are consistent with early observations and model simulations.

[20] Although good agreement was found between the lidar and SABER results, there are some differences in both upper stratosphere and upper mesosphere. These differences could be due to the tidal aliasing of the temperature AO and SAO derived from nighttime only lidar data, lidar temperature analysis algorithms, and the difference in sampling data between ground-based and space-based instruments, and the length of data set, as well as the larger uncertainties at the higher altitudes.

[21] Using the migrating tidal results extracted from the SABER analysis, we assess the tidal aliasing to lidar temperature AO and SAO by evaluating the seasonal oscillations of tides. The seasonal oscillations of tidal amplitudes are revealed to be generally less than 2 K below 80 km. However, at TMF (34°N) the AO oscillation of diurnal amplitude is increased to ~2.3 K near 75 km, corresponding to the large temperature AO difference between lidar and SABER, and also in phase with temperature AO. This positive correlation suggests the possible diurnal aliasing to the lidar results. The further analysis on the diurnal phase and lidar sampling local time indicates that the AO oscillation induced solely by migrating diurnal tide could reach as high as ~2 K near 75 km at TMF. This should be able to reduce the difference between lidar and

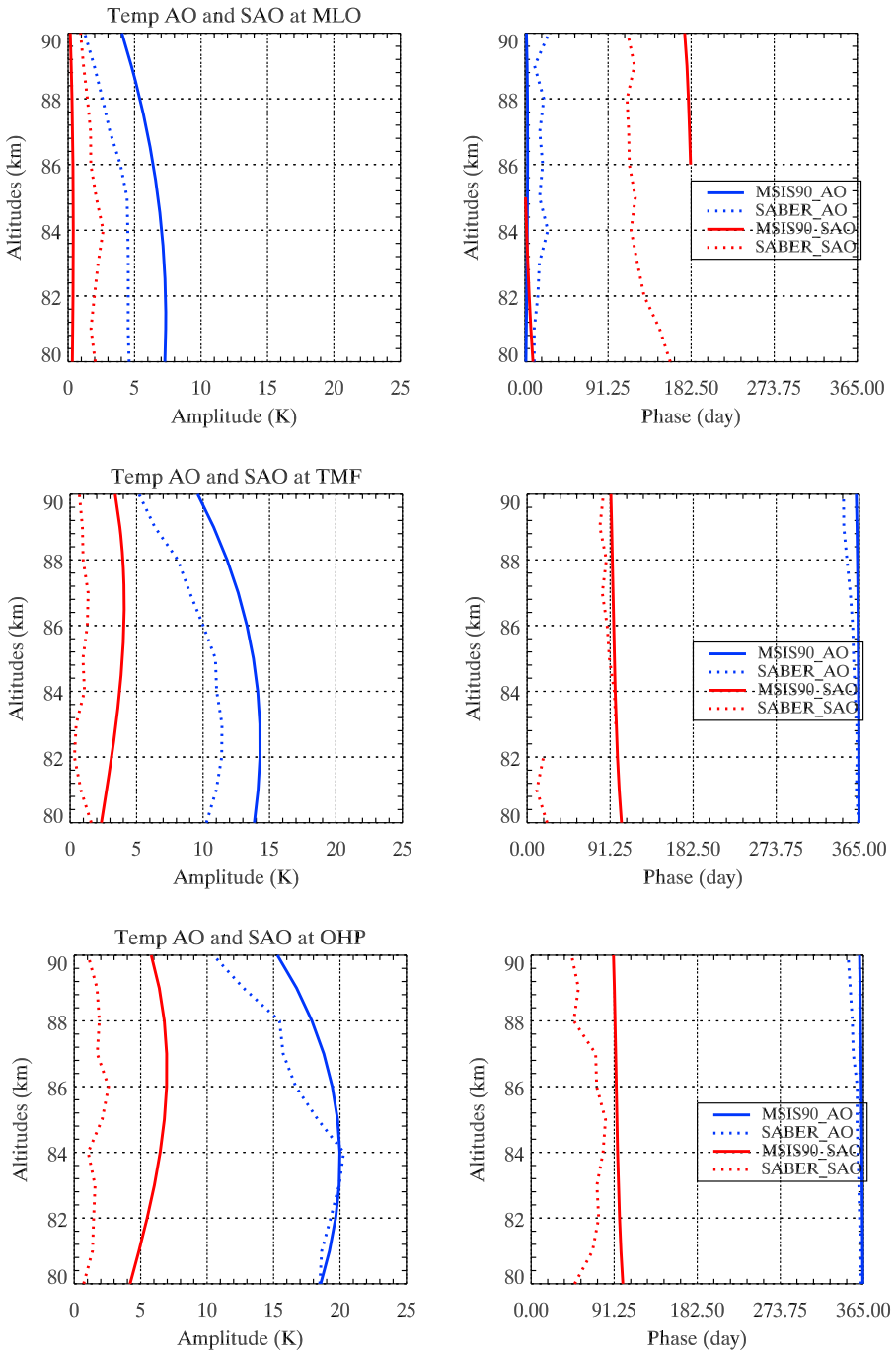

Figure 7. The temperature AO (blue lines) and SAO (red lines) derived from MSIS model (solid lines) and SABER (dotted lines) between 80 and 90 km at (top) MLO, (middle) TMF, and (bottom) OHP.

SABER derived temperature AO amplitudes. Similar statements could be applied to OHP site as well. At other sites, the tidal amplitude oscillations are quite small. In addition to the tidal aliasing, the possibly unrealistic seasonal oscillations embedded in the climatological models at reference point for lidar temperature analysis may also affect the lidar results on the top part of the profiles. The larger seasonal oscillations of the MSIS-90 model compared to SABER results suggest that these unrealistic oscillations may cause extra aliasing to the lidar derived temperature SAO below 80 km.

[22] **Acknowledgments.** The work described in this paper was carried out at the University of Science and Technology of China with the support of Chinese Academy of Sciences (CAS) KIP Pilot project kzcx2-yw-123, National Natural Sciences Foundation of China (NSFC) funds 40674087 and 40890165, China Meteorological Administration grant GYHY20070613, NSFC fund 40974084, and the CAS One Hundred Talent Program. The lidar temperature data are archived at the NDACC Data and Handling Facility and are publicly available (see http://www.ndacc.org). We acknowledge the support of the European Commission through the GEOMON Integrated Project under the Sixth Framework Program (contract FOP6-2005-Global-4-036677). The National Center for Atmospheric Research is operated by the University Corporation for Atmospheric Research under the sponsorship of the National Science Foundation.

References

Baldwin, M. P., et al. (2001), The quasi-biennial oscillation, *Rev. Geophys.*, *39*, 179–229, doi:10.1029/1999RG000073.

Baray, J.-L., J. Leveau, J. Porteneuve, G. Ancellet, P. Keckhut, F. Posny, and S. Baldy (1999), Description and evaluation of a tropospheric ozone lidar implemented on an existing lidar in the southern subtropics, *Appl. Opt.*, *38*, 6808–6817, doi:10.1364/AO.38.006808.

Crary, D. J., and J. M. Forbes (1983), On the extraction of tidal information from measurements covering a fraction of a day, *Geophys. Res. Lett.*, *10*, 580–582, doi:10.1029/GL010i007p00580.

Delisi, D. P., and T. J. Dunkerton (1988), Equatorial semiannual oscillation in zonally averaged temperature observed by the Nimbus 7 SAMS and LIMS, *J. Geophys. Res.*, *93*, 3899–3904, doi:10.1029/JD093iD04p03899.

Dunkerton, T. J. (1982), Theory of the mesopause semiannual oscillation, *J. Atmos. Sci.*, *39*, 2681–2690, doi:10.1175/1520-0469(1982)039<2681:TOTMSO>2.0.CO;2.

Forbes, J. M. (1995), Tidal and planetary waves, in *The Upper Mesosphere and Lower Thermosphere: A Review of Experiment and Theory*, *Geophys. Monogr. Ser.*, vol. 87, edited by R. M. Johnson and T. L. Killeen, pp. 67–87, AGU, Washington, D. C.

Garcia, R. R., and R. T. Clancy (1990), Seasonal variation in equatorial mesospheric temperatures observed by SME, *J. Atmos. Sci.*, *47*, 1666–1673, doi:10.1175/1520-0469(1990)047<1666:SVIEMT>2.0.CO;2.

Garcia, R. R., T. J. Dunkerton, R. S. Lieberman, and R. A. Vincent (1997), Climatology of the semiannual oscillation of the tropical middle atmosphere, *J. Geophys. Res.*, *102*, 26,019–26,032, doi:10.1029/97JD00207.

Haefele, A., K. Hocke, N. Kämpfer, P. Keckhut, M. Marchand, S. Bekki, B. Morel, T. Egorova, and E. Rozanov (2008), Diurnal changes in middle atmospheric H_2O and O_3: Observations in the Alpine region and climate models, *J. Geophys. Res.*, *113*, D17303, doi:10.1029/2008JD009892.

Hagan, M. E., and J. M. Forbes (2002), Migrating and nonmigrating diurnal tides in the middle and upper atmosphere excited by tropospheric latent heat release, *J. Geophys. Res.*, *107*(D24), 4754, doi:10.1029/2001JD001236.

Hamilton, K. (1982), Rocketsonde observations of the mesospheric semiannual oscillation at Kwajalein, *Atmos. Ocean*, *20*, 281–286.

Hauchecorne, A., and M. L. Chanin (1980), Density and temperature profiles obtained by lidar between 35 and 70 km, *Geophys. Res. Lett.*, *7*, 565–568, doi:10.1029/GL007i008p00565.

Hirota, I. (1978), Equatorial waves in the upper stratosphere and mesosphere in relation to the semi-annual oscillation of the zonal wind, *J. Atmos. Sci.*, *35*, 714–722, doi:10.1175/1520-0469(1978)035<0714:EWITUS>2.0.CO;2.

Keckhut, P., et al. (1996), Semidiurnal and diurnal temperature tides (30–55 km): Climatology and effect on UARS-LIDAR data comparisons, *J. Geophys. Res.*, *101*, 10,299–10,310, doi:10.1029/96JD00344.

Keckhut, P., et al. (2004), Review of ozone and temperature lidar validations performed within the framework of the network for the detection of stratospheric change, *J. Environ. Monit.*, *6*, 721–733, doi:10.1039/b404256e.

Leblanc, T., I. S. McDermid, P. Keckhut, A. Hauchecorne, C. Y. She, and D. A. Krueger (1998a), Temperature climatology of the middle atmosphere from long-term lidar measurements at middle and low latitudes, *J. Geophys. Res.*, *103*, 17,191–17,204, doi:10.1029/98JD01347.

Leblanc, T., I. S. McDermid, A. Hauchecorne, and P. Keckhut (1998b), Evaluation and optimization of lidar temperature analysis algorithms using simulated data, *J. Geophys. Res.*, *103*, 6177–6189, doi:10.1029/97JD03494.

Leblanc, T., I. S. McDermid, and D. A. Ortland (1999), Lidar observations of the middle atmospheric thermal tides and comparison with the High Resolution Doppler Imager and Global-Scale Wave Model: 1. Methodology and winter observations at Table Mountain (34.4°N), *J. Geophys. Res.*, *104*, 11,917–11,929.

Li, T., T. Leblanc, and I. S. McDermid (2008a), Interannual variations of middle atmospheric temperature as measured by the JPL lidar at Mauna Loa Observatory, Hawaii (19.5°N, 155.6°W), *J. Geophys. Res.*, *113*, D14109, doi:10.1029/2007JD009764.

Li, T., C.-Y. She, S. E. Palo, Q. Wu, H.-L. Liu, and M. L. Salby (2008b), Coordinated lidar and TIMED observations of the quasi-two-day wave during August 2002–2004 and possible quasi-biennial oscillation influence, *Adv. Space Res.*, *41*(9), 1463–1470, doi:10.1016/j.asr.2007.03.052.

McDermid, I. S., T. D. Walsh, A. Deslis, and M. While (1995), Optical systems design for a stratospheric lidar system, *Appl. Opt.*, *34*, 6201–6210, doi:10.1364/AO.34.006201.

Morel, B., H. Bencherif, P. Keckhut, S. Baldy, and A. Hauchecorne (2002), Evidence of tidal perturbations in the middle atmosphere over southern tropics as observed by Rayleigh lidar, *J. Atmos. Sol. Terr. Phys.*, *64*, 1979–1988, doi:10.1016/S1364-6826(02)00223-7.

Randel, W. J., et al. (2004), The SPARC intercomparison of middle-atmosphere climatologies, *J. Clim.*, *17*, 986–1003, doi:10.1175/1520-0442(2004)017<0986:TSIOMC>2.0.CO;2.

Reed, R. J. (1962), Some features of the annual temperature regime in the tropical stratosphere, *Mon. Weather Rev.*, *90*, 211–215, doi:10.1175/1520-0493(1962)090<0211:SFOTAT>2.0.CO;2.

Remsberg, E. E., P. P. Bhatt, and L. E. Deaver (2002), Seasonal and longer-term variations in middle atmosphere temperature from HALOE on UARS, *J. Geophys. Res.*, *107*(D19), 4411, doi:10.1029/2001JD001366.

Remsberg, E., G. Lingenfelser, V. L. Harvey, W. Grose, J. Russell III, M. Mlynczak, L. Gordley, and B. T. Marshall (2003), On the verification of the quality of SABER temperature, geopotential height, and wind fields by comparison with Met Office assimilated analyses, *J. Geophys. Res.*, *108*(D20), 4628, doi:10.1029/2003JD003720.

Richter, J. H., and R. R. Garcia (2006), On the forcing of the Mesospheric Semi-Annual Oscillation in the Whole Atmosphere Community Climate Model, *Geophys. Res. Lett.*, *33*, L01806, doi:10.1029/2005GL024378.

Russell, J. M., III, et al. (1999), An overview of the SABER experiment and preliminary calibration results, *Proc. SPIE Int. Soc. Opt. Eng.*, *3756*, 277–288.

Sassi, F., and R. R. Garcia (1997), The role of equatorial waves forced by convection in the tropical semiannual oscillation, *J. Atmos. Sci.*, *54*, 1925–1942, doi:10.1175/1520-0469(1997)054<1925:TROEWF>2.0.CO;2.

Xu, J., A. K. Smith, W. Yuan, H.-L. Liu, Q. Wu, M. G. Mlynczak, and J. M. Russell III (2007), Global structure and long-term variations of zonal mean temperature observed by TIMED/SABER, *J. Geophys. Res.*, *112*, D24106, doi:10.1029/2007JD008546.

Zhang, X., J. M. Forbes, M. E. Hagan, J. M. Russell III, S. E. Palo, C. J. Mertens, and M. G. Mlynczak (2006), Monthly tidal temperatures 20–120 km from TIMED/SABER, *J. Geophys. Res.*, *111*, A10S08, doi:10.1029/2005JA011504.

Zhao, Y., M. J. Taylor, H.-L. Liu, and R. G. Roble (2007), Seasonal oscillations in mesospheric temperatures at low-latitudes, *J. Atmos. Sol. Terr. Phys.*, *69*, 2367–2378, doi:10.1016/j.jastp.2007.07.010.

H. Bencherif, Laboratoire de l'Atmosphère et des Cyclones, Université de La Réunion, BP 7151, F-97715 Saint-Denis, France.

X. Dou, T. Li, S. Wang, and X. Xue, Mengcheng National Geophysical Observatory, School of Earth and Space Sciences, University of Science and Technology of China, 96 Jinzhai Road, Hefei, Anhui 230026, China. (litao@ustc.edu.cn)

A. Hauchecorne and P. Keckhut, Service d'Aéronomie, Institut Pierre-Simon Laplace, CNRS, BP 3, Route des Gatines, F-91371 Verrières-le-Buisson, France.

C. Heinselman, SRI International, 333 Ravenswood Avenue, Menlo Park, CA 94025-3493, USA.

T. Leblanc and I. S. McDermid, Table Mountain Facility, Jet Propulsion Laboratory, California Institute of Technology, Wrightwood, CA 92397, USA.

H.-L. Liu, High Altitude Observatory, National Center for Atmospheric Research, Boulder, CO 80301, USA.

M. G. Mlynczak, NASA Langley Research Center, Hampton, VA 23681, USA.

J. M. Russell III, Center for Atmospheric Sciences, Hampton University, Hampton, VA 23668, USA.

W. Steinbrecht, Meteorological Observatory Hohenpeissenberg, German Weather Service, Albin Schwaiger Weg 10, D-82383 Hohenpeissenberg, Germany.

J. Xu, Key Laboratory for Space Weather, Chinese Academy of Sciences, Beijing 100080, China.